386 KSME International Journal, Vol. 11, No. 4, pp. 386~396, 1997

An Efficient and Accurate Dynamic Stress Computation by Flexible Multibody Dynamic System Simulation and Reanalysis

Jeha Ryu*, Ho-Soo Kim* and Hong Jae Yim**

(Received August 3, 1996)

This paper presents an efficient and accurate method for dynamic stress computation based on reanalysis in flexible multibody dynamic system simulation. The mode-acceleration concept that is widely used in linear strucural dynamics was utilized for accuracy improvement. A mode-acceleration equation for each flexible body is defined and the load term in the right hand side of the equation is represented as a combination of space-dependent and time-dependent terms so that efficient computations of dynamic stresses can be achieved. The load term is obtained from dynamic simulation of a flexible multibody system and a finite element method is used to compute stresses by quasi-static analyses. A numerical example of a flexible four-bar mechanism shows effectiveness of the proposed method for flexible multibody dynamic systems such as linkages and vehicle systems.

Key Words: Flexible Multibody Dynamic System Simulation, Dynamic Stress History, Mode-Acceleration Method, Mode-Displacement Method

1. Introduction

Design of a mechanical system subject to dynamic loads requires extensive engineering study on performance of the system before a prototype is built and tested. When components of a mechanical system are considered to be deformable, dynamic analyses have been carried out to obtain dynamic stress histories at points of interest for fatigue life prediction and stress-safe design. Fatigue failure may result from high stress levels together with the large number of stress reversals when millions of cycles of dynamic loads are applied to a machine component in a dynamic system. Even in a few cycles of dynamic loads, a machine component may fail because of the excessive stresses resulting from large magnitude loads. Therefore, an accurate prediction of dynamic stress histories is a keystone for fatigue life prediction and stress-safe design.

Dynamic stress histories have been computed by high speed digital computers to accelerate design cycles in the design of flexible multibody systems. These computer-based approaches can be categorized into four groups: *Rigid Body Dynamic Simulation combined with Quasi-static Finite Element Method* (Winfrey, 1971, Sadler and Sandor, 1973), *Finite Element Nodal Approach* (Turcic and Midha, 1984a, Nagarajan and Turcic, 1990, Yang and Sadler, 1990), *Modal Stress Superposition Method* (Liu, 1987), and *Hybrid Method* (Yim and Lee, 1996).

In the area of linear structural dynamics (Craig, 1981), the *Mode-Acceleration Method* (MAM) has been used to improve dynamic solutions by static structural analyses after modal velocities and accelerations are obtatined by the *Mode-Displacement Method* (MDM). This method used a truncated set of normal modes to appoximate the dynamic responses. In the area of nonlinear flexible multibody dynamics, on the other hand,

* Department of Mechatronics, Kwangju Institute of Science and Technology 572 Sangam-dong, Kwangsan-ku, Kwangju, 506-712, Korea
** Department of Mechanics and Design, Kookmin University 861-1, Jeongneung-dong, Sungbuk-ku, Seou, 136-702, Korea

the hybrid method (Yim and Lee, 1996) improves accuracy of the dynamic stresses by utilizing the dynamic loads obtained from flexible multibody dynamic simulations that used the assumed mode superposition method. However, the amount of computation in the hybrid method is tremendous for accurate stress calculation because the required number of quasi-static stress analyses corresponding to the inertia loads that are distributed over all finite element nodes increases greatly as the total number of nodal points increases. Therefore, an efficient method should be sought out.

The objective of this paper is to present an efficient method of improving the accuracy of dynamic stresses that are obtained from the conventional flexible multibody dynamic analysis that uses the assumed mode superposition method. By utilizing the concept of the MAM in linear structural dyanmics, we explain theoretically how the proposed MAM improves the accuracy of dynamic stresses. Finally, an efficient computational method is summarized to solve the mode-acceleration equations in flexible multibody dynamic systems.

This paper is organized as follows: Section 2 summarizes basic ideas and mathematical derivations of the MDM and the MAM in linear structural dynamics and explains the reason why the MAM improves the the accuracy of dynamic stresses. Section 3 derives mode-acceleration equations for a flexible body in the nonlinear flexible multibody dynamic systems from the variational Cartesian equations of motion of the body. Section 4 summarizes a computationally efficient method of solving the mode-acceleration equations. Section 5 presents a numerical example to show the effectiveness of the proposed method and it is followed by conclusions in Sec. 6.

2. MDM vs MAM in Linear Structural Dynamics

Two versions of the mode superposition method have been used in the dynamic analysis of linear structures: (1) the *mode-displacement method* (MDM), and (2) the *mode-acceleration method* (MAM). Both methods use a truncated set of eigenvectors as bases to approximate the response of the structure.

Consider an undamped n degree-of-freedom linear dynamic system. In matrix form, the dynamic equations are given by

$$\boldsymbol{M}\ddot{\boldsymbol{U}}+\boldsymbol{K}\boldsymbol{U}=\boldsymbol{F}(t) \tag{1}$$

where $\boldsymbol{M}$ and $\boldsymbol{K}$ are the $(n\times n)$ mass and stiffness matrices of the structure, respectively; and $\ddot{\boldsymbol{U}}$, $\boldsymbol{U}$ and $\boldsymbol{F}(t)$ are the nodal acceleration, displacement, and force vectors, respectively.

Equation (1) can be transformed to a set of n uncoupled equations by the following transformation,

$$\boldsymbol{U}=\boldsymbol{\Phi}\boldsymbol{a}(t)=\sum_{i=1}^{n}\boldsymbol{\phi}_i a_i(t) \tag{2}$$

where $\boldsymbol{a}(t)$ is the modal coordinate vector and $\boldsymbol{\Phi}$ is the modal matrix whose i-th column vectors $\boldsymbol{\phi}_i$ are the orthonormalized eigenvectors of the system satisfying the eigenvalue problem :

$$\boldsymbol{K}\boldsymbol{\phi}_i=\omega_i^2\boldsymbol{M}\boldsymbol{\phi}_i \tag{3}$$

where ω_i is the i-th natural frequency. Then, Eq. (1) can be rewritten as

$$\ddot{\boldsymbol{a}}+\boldsymbol{\Lambda}\boldsymbol{a}=\boldsymbol{f}(t) \tag{4}$$

where matrix $\boldsymbol{\Lambda}$ is a diagonal matrix that is composed of the square of natural frequencies. The following equations are used in deriving Eq. (4) from Eq. (1).

$$\boldsymbol{\Phi}^T\boldsymbol{M}\boldsymbol{\Phi}=\boldsymbol{I} \tag{5}$$

$$\boldsymbol{K}\boldsymbol{\Phi}=\boldsymbol{M}\boldsymbol{\Phi}\boldsymbol{\Lambda} \tag{6}$$

$$\boldsymbol{\Phi}^T\boldsymbol{F}(t)=\boldsymbol{f}(t) \tag{7}$$

In the traditional MDM, after the modal coordinate history $a_i(t)$ $(i=1, \cdots, m)$ is computed from Eq. (4), the mode-displacement solution is obtained approximately as

$$\hat{\boldsymbol{U}}(t)=\sum_{i=1}^{m}\boldsymbol{\phi}_i a_i(t) \tag{8}$$

where m is the number of normal modes, and is generally much smaller than the total degrees of freedom n. Therefore, the MDM neglects completely the normal modes from $(m+1)$ to n.

The MAM, first proposed by Williams (1945), compensates for the effect of neglected high frequency modes. Bisplinghoff Ashley (1955) and Thomson(1972) insisted that the MAM has better convergence characteristics and requires fewer modes than the MDM. More recent versions of the MAM in the literature include Maddox (1975), Hangsteen and Bell (1979), and Cornwell, Craig, and Johnson(1983). The classical mode-acceleration method can be derived by solving Eq. (1) for U:

$$\boldsymbol{U}=\boldsymbol{K}^{-1}\boldsymbol{F}-\boldsymbol{K}^{-1}\boldsymbol{M}\ddot{\boldsymbol{U}} \tag{9}$$

where is is assumed without loss of generality that the stiffness matrix is nonsingular. In other words, rigid body modes are not considered. If a truncated set of m normal modes is used to approximate the nodal acceleration, the second term of the right side in Eq. (9) can be written as

$$\boldsymbol{K}^{-1}\boldsymbol{M}\ddot{\boldsymbol{U}}(t)\cong\boldsymbol{K}^{-1}\boldsymbol{M}\hat{\boldsymbol{\Phi}}\ddot{\hat{\boldsymbol{a}}}(t) \tag{10}$$

where $\hat{\boldsymbol{\Phi}}$ and $\ddot{\hat{\boldsymbol{a}}}(t)$ are the truncated $(n\times m)$ modal matrix and the $(m\times 1)$ modal coordinate acceleration vector, respectively. Using the relationship derived from Eq. (6),

$$\boldsymbol{K}^{-1}\boldsymbol{M}\hat{\boldsymbol{\Phi}}=\hat{\boldsymbol{\Phi}}\hat{\boldsymbol{\Lambda}}^{-1} \tag{11}$$

where $\hat{\Lambda}$ is the $(m\times m)$ diagonal matrix that is composed of the square of m natural frequencies, the mode-accleration solution $\overline{U}$ is given by

$$\overline{\boldsymbol{U}}=\boldsymbol{K}^{-1}\boldsymbol{F}(t)-\hat{\boldsymbol{\Phi}}\hat{\boldsymbol{\Lambda}}^{-1}\ddot{\hat{\boldsymbol{a}}}(t) \tag{12}$$

The first term in the right side of Eq. (12) accounts for the contribution of higher modes by implicitly considering a complete set of n modes. This term is the pseudo-static response that is equivalent to carrying out a static analysis at each time step. The second term in the right side of Eq. (12) represents a dynamic correction applied to the pseudo-static response and gives the method its name, the mode-acceleration method. Once the $(m\times 1)$ vector $\ddot{\hat{\boldsymbol{a}}}(t)$ is obtained by Eq. (4), it is easy to obtain the mode-accleration solution by Eq. (12), which is a quasi-static equation.

In order to show more explicitly that the MAM improves dynamic solutions obtained by the MDM, consider a computational variant that is obtained by expanding the flexibility matrix in terms of a truncated eigenbasis(Léger and Wilson, 1988). Solution of Eq. (4) for $\ddot{\hat{\boldsymbol{a}}}(t)$ gives

$$\ddot{\hat{\boldsymbol{a}}}(t)=\hat{\boldsymbol{\Phi}}^{T}\boldsymbol{F}(t)-\hat{\boldsymbol{\Lambda}}\hat{\boldsymbol{a}}(t) \tag{13}$$

Inserting Eq. (13) into Eq. (12) gives

$$\overline{\boldsymbol{U}}=\boldsymbol{K}^{-1}\boldsymbol{F}(t)+\hat{\boldsymbol{\Phi}}\hat{\boldsymbol{a}}(t)-\hat{\boldsymbol{\Phi}}\hat{\boldsymbol{\Lambda}}^{-1}\hat{\boldsymbol{\Phi}}^{T}\boldsymbol{F}(t) \tag{14}$$

This equation can be written as

$$\overline{\boldsymbol{U}}=\hat{\boldsymbol{\Phi}}\hat{\boldsymbol{a}}(t)+(\boldsymbol{K}^{-1}-\hat{\boldsymbol{\Phi}}\hat{\boldsymbol{\Lambda}}^{-1}\hat{\boldsymbol{\Phi}}^{T})\boldsymbol{F}(t) \tag{15}$$

Equation (15) is then rewritten as

$$\overline{\boldsymbol{U}}=\hat{\boldsymbol{U}}(t)+(\boldsymbol{K}^{-1}-\boldsymbol{K}_m^{-1})\boldsymbol{F}(t) \tag{16}$$

In this final expression, the first term corresponds to the conventional mode-displacement solution, and the second term represents the additional static correction, i.e., the amount of improvement by the MAM in deflections, where $\boldsymbol{K}_m^{-1}$ is a symbolic representation for the truncated expansion of the flexibility matrix using a reduced set of m eigenvectors. Note that this static correction concept has been used in the context of dynamic substructuring to improve the convergence of structural responses computed by component mode synthesis (Craig and Chang, 1977). The static correction vector is defined as the residual attachment mode obtained from the application of the residual flexibility matrix $(\boldsymbol{K}^{-1}-\boldsymbol{K}_m^{-1})$ to the specified unit magnitude loading.

In addition to determining the displacement history, a dynamic analysis usually determine stress histories(e.g., moment, shear, axial stress, etc.) or at least the maximum values of stress at specified locations in the structure. The following are symbolic representations of stresses obtained by mode-superposition. For the MDM,

$$\hat{\boldsymbol{\sigma}}(t)=\sum_{i=1}^{m}\boldsymbol{s}_i\boldsymbol{a}_i \tag{17}$$

where $\boldsymbol{s}_i$ is the stress influence coefficient that is the contribution to the stress vector $\hat{\boldsymbol{\sigma}}$ due to a unit displacement of the i-th mode, i.e., $a_i=1$. Note and the modal stress superposition method (Liu, 1987) used the same principle in the flexible multibody dynamics. For the MAM, the displacement approximation in Eq. (12) leads to the stress approximation

$$\overline{\boldsymbol{\sigma}}(t)=\boldsymbol{\sigma}_{\text{pseudostatic}}-\sum_{i=1}^{m}\boldsymbol{s}_i\frac{\ddot{a}_i}{\omega_i^2} \tag{18}$$

Higher modes are increasingly more important for moments and shears than for deflections (Craig, 1981). Therefore, the MAM is particularly beneficial in speeding up the convergence of the internal stresses computation.

3. MDM vs MAM in Nonlinear Flexible Multibody Dynamics

3.1 Variational equations of motion of a flexible body

Consider a flexible body that is in dynamic equilibrium in a deformed configuration, as shown in Fig. 1. In the figure, the $\underline{X}$-$\underline{Y}$-$\underline{Z}$ coordinate system is the inertial reference frame and the x-y-z coordinate system is the body fixed reference frame in an undeformed configuration. An underlined variable is measured in the inertial reference frame, while other variables are measured in the local body fixed reference frame.

The variational equation of motion of a flexible body are given as (Wu et al., 1989)

$$\int_S \delta \boldsymbol{r}^{pT} \boldsymbol{T}^p dS - \int_V \delta \boldsymbol{r}^{pT} \{ \rho \ddot{\boldsymbol{r}}^p - \boldsymbol{f}^p \} dV = \int_V \delta \boldsymbol{\varepsilon}^{pT} \boldsymbol{\tau}^p dV \tag{19}$$

where $\delta \boldsymbol{r}^p$ is the virtual displacement vector of point p that is consitent with constraints; $\boldsymbol{T}^p$ is a surface traction vector at point p; ρ is the mass density, $\ddot{\boldsymbol{r}}^p$ is the acceleration vector of point p; $\boldsymbol{f}^p$ is the body force vector at point p; $\boldsymbol{\tau}^p$ is the (6×1) stress vector, $\delta \boldsymbol{\varepsilon}^p$ is the variation of the (6×1) strain vector consistent with given boundary conditions; and V and S are the volume and surface of the body before it is deformed. Dots over a vector in Eq. (19) and in the following derivations denote the total differentiation with respect to time. Note that every vector is represented with respect to the body fixed reference frame; i.e., for any arbitrary vector, $\boldsymbol{v} = \boldsymbol{A}^T \underline{\boldsymbol{v}}$, where $\boldsymbol{A}$ is the orientation matrix of the body fixed reference frame.

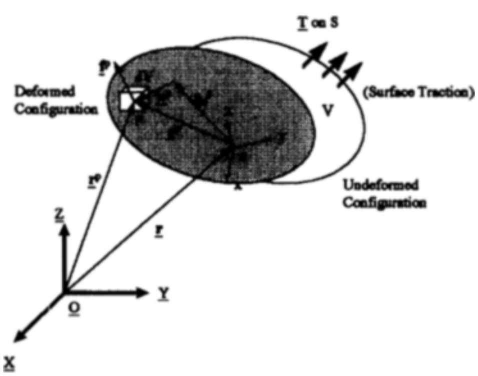

Fig. 1 Underformed and deformed configurations of a flexible body

By using relationship $\boldsymbol{s}^p = \boldsymbol{s}_0^p + \boldsymbol{u}^p$, the virtual displacement and the acclecation vectors of point p are represented in the body fixed reference frame as

$$\delta \boldsymbol{r}^p = \delta \boldsymbol{r} - \tilde{\boldsymbol{s}}^p \delta \boldsymbol{\pi} + \delta \boldsymbol{u} \tag{20}$$

$$\ddot{\boldsymbol{r}}^p = \ddot{\boldsymbol{r}} + (\tilde{\boldsymbol{\omega}}\tilde{\boldsymbol{\omega}} + \dot{\tilde{\boldsymbol{\omega}}}) \boldsymbol{s}_0^p + (\tilde{\boldsymbol{\omega}}\tilde{\boldsymbol{\omega}} + \dot{\tilde{\boldsymbol{\omega}}}) \boldsymbol{u} + 2\tilde{\boldsymbol{\omega}} \dot{\boldsymbol{u}} + \ddot{\boldsymbol{u}} \tag{21}$$

where $\delta \boldsymbol{r}$, $\delta \boldsymbol{\pi}$, and $\delta \boldsymbol{u}$ are the variation of the position, orientation, and deformation vectors, repectively; and $\ddot{\boldsymbol{r}}$, $\dot{\boldsymbol{\omega}}$, and $\boldsymbol{\omega}$ are the translational and rotational acceleration and angular Velocity Vectors of the body fixed reference frame, respectively. Note that the superscript p on $\boldsymbol{u}$ is omitted to simplify notation. Note also that the ~ (tilde) operator over a vector gives a (3×3) skew -symmatric matrix.

Substitution of Eqs. (20) and (21) into Eq. (19) gives

$$\begin{aligned} \delta \boldsymbol{q}_R^T \Big[\int_S \boldsymbol{Q}_{RT} dS - \int_V \{ \rho (\boldsymbol{M}_{RR} \ddot{\boldsymbol{q}}_R + \boldsymbol{M}_{RF} \ddot{\boldsymbol{u}} + \boldsymbol{S}_{RR}) \\ - \boldsymbol{Q}_{Rf} \} dV + \int_S \delta \boldsymbol{u}^T \boldsymbol{T}^p dS \\ - \int_V \delta \boldsymbol{u}^T \{ \rho (\ddot{\boldsymbol{u}} + \boldsymbol{M}_{RF}^T \ddot{\boldsymbol{q}}_R + \boldsymbol{S}_{FF}) \\ - \boldsymbol{f}^p \} dV = \int_V \delta \boldsymbol{\varepsilon}^{pT} \boldsymbol{\tau}^p dV \end{aligned} \tag{22}$$

Terms in Eq. (22) are defined as

$$\delta \boldsymbol{q}_R^T = [\delta \boldsymbol{r}^T, \delta \boldsymbol{\pi}^T] \tag{23}$$

$$\ddot{\boldsymbol{q}}_R^T = [\ddot{\boldsymbol{r}}^T, \dot{\boldsymbol{\omega}}^T] \tag{24}$$

$$\boldsymbol{M}_{RR} = \begin{bmatrix} \boldsymbol{I} & -\tilde{\boldsymbol{s}}^P \\ \tilde{\boldsymbol{s}}^p & -\tilde{\boldsymbol{s}}^P \tilde{\boldsymbol{s}}^P \end{bmatrix} \tag{25}$$

$$\boldsymbol{M}_{RF} = \begin{bmatrix} \boldsymbol{I} \\ \tilde{\boldsymbol{s}}^P \end{bmatrix} \tag{26}$$

$$\boldsymbol{S}_{RR} = \begin{bmatrix} \tilde{\boldsymbol{\omega}}\tilde{\boldsymbol{\omega}} \boldsymbol{s}^P + 2\tilde{\boldsymbol{\omega}} \dot{\boldsymbol{u}} \\ \tilde{\boldsymbol{s}}^P \tilde{\boldsymbol{\omega}}\tilde{\boldsymbol{\omega}} \boldsymbol{s}^P + 2\tilde{\boldsymbol{s}}^P \tilde{\boldsymbol{\omega}} \dot{\boldsymbol{u}} \end{bmatrix} \tag{27}$$

$$Q_{RF}=\begin{bmatrix} f^P \\ \tilde{s}^P f^P \end{bmatrix} \quad (28)$$

$$Q_{RT}=\begin{bmatrix} T^P \\ \tilde{s}^P T^P \end{bmatrix} \quad (29)$$

$$S_{FF}=\tilde{\omega}\tilde{\omega}s^p+2\tilde{\omega}\dot{u} \quad (30)$$

where I is a (3×3) identity matrix.

If the surface traction vector T^P includes constraint reaction loads that are obtained through Lagrangian multipliers associated with constraints, then δq_R^T in Eq. (22) is arbitrary. Therefore, Eq. (22) is divided into (6×1) vector equations for gross body motion and a variational equation for deformation as,

$$\int_S Q_{RT}dS-\int_V\{\rho(M_{RR}\ddot{q}_R+M_{RF}\ddot{u}+S_{RR})-Q_{Rf}\}dV=0 \quad (31)$$

$$\int_S\delta u^T T^P dS-\int_V\delta u^T\{\rho(\ddot{u}+M_{RF}^T\ddot{q}_R+S_{FF})-f^p\}dV=\int_V\delta\varepsilon^{pT}\tau^p dV \quad (32)$$

Equation (32) means that, for a flexible component a flexible multibody system, internal loads, D'Alembert inertial loads, applied loads, and constraint reaction loads are self-equilibrated at each time step t during the motion of the flexible multibody system. Note that even though Eq. (32) is written for a flexible body in a multibody system, geometrically nonlinear coupling effects from gross body motion and elastic deformation are taken into account during dynamic simulation of a flexible multibody system. Note also that Eq. (31), which is the equilibrium equation for the gross body motion, is also satisfied during the motion.

3.2 Mode-displacement and mode-acceleration solutions in flexible multibody dynamics

Dynamic simulation of a flexible multibody system can be performed by representing the elastic displacement field u of a flexible component as the sum of modal coordinates multiplied by assumed modes, which may be a truncated set of normal modes and/or static correction modes (Yoo and Haug, 1986). Normal modes of a flexible component are obtained by solving the eigenvalue problem in Eq. (3) for a few of the lowest frequency vibration modes. These free vibration modes represent deformation shapes of the component due to its mass and stiffness distribution. To represent the local deformation at the action point of constraint and applied loads, static correction modes, such as attachment modes (Craig and Chang, 1977) or constraint modes (Craig and Bampton, 1986), can be used together with the vibration normal modes. For example, an attachment mode is defined by imposing a unit force in the direction of one physical coordinate of the flexible component, and zero forces elsewhere.

With the assumed-mode representation of the elastic displacement field of each flexible component, system equations of motion of a flexible multibody system are constructed by assembling variational equations of motion (Eqs. (31) and (32)) of each flexible body in the system. The mode-displcement solutions are then obtained from the dynamic simulation of the system by solving and by integrating the system equations of motion (Wu et al., 1989). In this case, elastic displacements ($\hat{U}$) and dynamic stresses ($\hat{\sigma}$) take the form of Eqs. (8) and (17), respectively. If only a truncated set of normal modes is used in the dynamic simulation of the system, then the effects of the truncated higher frequency modes are totally neglected, as in linear structural dynamics.

On the other hand, mode-acceleration solutions can be obtained as follows: Rearrangement of Eq. (32) yields

$$\int_V\delta u^T\rho\{\ddot{u}+2\tilde{\omega}\dot{u}+(\tilde{\omega}\tilde{\omega}+\dot{\tilde{\omega}})u\}dV+\int_V\delta\varepsilon^{pT}\tau^p dV$$
$$=\int_S\delta u^T T^P dS+\int_V\delta u^T f^p dV-\int_V\delta u^T\rho\{\ddot{r}+(\tilde{\omega}\tilde{\omega}+\dot{\tilde{\omega}})s_0^p\}dV \quad (33)$$

If Eq. (33) is projected into a finite element equilibrium equation according to the standard discretization and assembly procedure by the direct stiffness method (Bathe, 1996), then it can be shown easily that Eq. (33) can be expressed symbolically as

$$\begin{aligned} & M\ddot{U} + C_c(t)\dot{U} + M_c(t)U + KU \\ & = F_T(t) + F_f(t) + F_i(s_0^p, \dot{r}, \omega, \dot{\omega}, t) \\ & \equiv F \end{aligned} \tag{34}$$

where M is the mass matrix of a flexible body; $C_c(t)$ and $M_c(t)$ are the time-varying matrices resulting from the coupling terms between the gross body motion and the elastic deformation; K is the stiffness matrix of the body, $\ddot{U}$, $\dot{U}$, and U are the time-varying nodal acceleration, velocity, and displacement vectors, respectively; and F_T, F_f, and F_i are the nodal force vectors generated from the surface traction loads, the applied body loads, and the distributed D'Alembert inertial loads resulting from the gross body motion, respectively. Note that the mass matrix M and the stiffness matrix K are time-invariant bacause they are constructed for single flexible component of the multibody system and because they are defined with respect to the body reference frame, which is fixed to the undeformed configuration of the flexible body.

If the nodal forces, accelerations, velocties, and displacements in the left side of Eq. (34) except KU are approximated by the mode-displacement solutions that are obtained by the dynamic simulation of a flexible multibody system, the mode-acceleration solutions in flexible multibody dynamics can be written as

$$\overline{U} = K^{-1}(F - M\ddot{\hat{U}} - C_c\dot{\hat{U}} - M_c\hat{U}) \tag{35}$$

Note that Eq. (35) is a quasi-static equation where every load is self-equilibrated. Dynamic stresses ($\overline{\sigma}$) are also computed from the quasi-static equation.

The fact that the proposed MAM improves the dynamic stresses obtained by the MDM can be easily explained in a similar way as in linear structural dynamics. For example, when only m truncated set of normal modes is used to describe an elastic deformation field of a flexible component in the dynamic simulation of a flexible multibody system, it can be shown easily that Eq. (35) can be rewritten as

$$\overline{U} = \hat{U} + G_d(F - C_c\dot{\hat{U}} - M_c\hat{U}) \tag{36}$$

where G_d is the residual flexibility matrix which is defined as $G_d \equiv (K^{-1} - K_m^{-1})$. Therefore, the mode-acceleration solutions improves the mode-displacement solutions by the addition of the static correction terms $G_d(F - C_c\dot{\hat{U}} - M_c\hat{U})$. Notice that if all normal modes are used, then the residual flexiblity matrix becomes zero, meaning that no improvement is achieved because the mode-acceleration solutions are the same as the mode-displacement solutions.

The basic computational procedure of the proposed method can be summarized as follows: First, obtain time histories of gross body motion, constraint reaction loads, and elastic deformation by approximating the elastic deformation field of a flexible component by a suitable set of modes, and by solving a coupled set of system equations of motion. Second, compute the nodal force vectors in the right hand side of Eq. (36) as is explained in Chapter 4 and solve the quasi-static equation to obtain improved dynamic stresses. The proposed MAM in flexible multibody dynamics compensates for the effect of neglected higher frequency vibration normal modes, the reason of which can be deduced from the explanation in linear structural dynamics in Chapter 2. Therefore, the method proposed in this paper generates more accurate dynamic stresses than does the modal stress superposition method (Liu, 1987).

4. Efficient Solution of Mode-Acceleration Equations

From Eq. (36), the mode-acceleration equations can be rewritten as

$$\begin{aligned} K\overline{U} = & (F_i(s_0^p, \dot{r}, \omega, \dot{\omega}) - M\ddot{\hat{U}} - C_c\dot{\hat{U}} \\ & - M_c\hat{U}) + F_T + F_f \end{aligned} \tag{37}$$

Even though the mode-acceleration equations are static linear equations, the solution of these equations is expensive because the load vectors in the right side of Eq. (37) contains numerous time-varying loads. This section presents an efficient method of solving the mode-acceleration equations using lumped mass approach for inertial forces that are terms in parenthesis in Eq. (37). First, the nodal force vectors are represented as a sum of products of space-dependent terms with time-dependent terms. Second, if a set of nodal loads associated with a unit value of a time-dependent term is applied statically to the finite element structural analysis model, a stress associated with this time-invariant load is obtained at the node of interest. This stress is defined as a stress influence coefficient associated with the time-dependent term. Third, the total resultant stress histories are generated by multiplying the actual magnitude of the time-dependent term with the stress influence coefficient and then by summing over all load cases. Note that even though a flexible body is moving in space, only one configuration of the structural analysis model is needed because (1) the local representation of kinematic varibles and loads are used and (2) modal coordinates are employed as generalized coordinates. This solution scheme is very efficient because it is based on the

superposition principle applicable to the time-invariant structural analysis. The following subsections summarize the solution procedure explained above for the inertial, constraint reaction, and applied forces.

4.1 Dynamic stresses by inertial force

Assume that a flexible body is discretized into finite elements and mass is lumped at each node appropriately. In the deformed configuration, D'Alembert inertial forces on a lumped mass m^p at point p can be expressed as

$$\boldsymbol{f}^p = \boldsymbol{f}_r^p + \boldsymbol{f}_d^p \tag{38}$$

Forces in Eq. (38) are defined as

$$\boldsymbol{f}_r^p = -m^p(\ddot{\boldsymbol{r}} + \tilde{\boldsymbol{\omega}}\tilde{\boldsymbol{\omega}}\boldsymbol{s}_0^p + \dot{\tilde{\boldsymbol{\omega}}}\boldsymbol{s}_0^p) \tag{39}$$

$$\boldsymbol{f}_d^p = -m^p\{(\tilde{\boldsymbol{\omega}}\tilde{\boldsymbol{\omega}} + \dot{\tilde{\boldsymbol{\omega}}})\boldsymbol{\Phi}^p\hat{\boldsymbol{a}} + 2\tilde{\boldsymbol{\omega}}\boldsymbol{\Phi}^p\dot{\hat{\boldsymbol{a}}} + \boldsymbol{\Phi}^p\ddot{\hat{\boldsymbol{a}}}\} \tag{40}$$

where $\boldsymbol{\Phi}^p$ is the $(3\times m)$ translational modal matrix defined at nodal point p and $\hat{\boldsymbol{a}}$, $\dot{\hat{\boldsymbol{a}}}$, and $\ddot{\hat{\boldsymbol{a}}}$ are modal displacement, velocity, and acceleration vectors that are generated from a dynamic simulation of flexible multibody systems. Note that $\boldsymbol{f}_r^p$ represents inertial forces resulting from the gross body motion, while $\boldsymbol{f}_d^p$ represents inertial forces resulting from the elastic deformation. Therefore, $\boldsymbol{F}_i$ in Eq. (37) is a nodal force vector generated from $\boldsymbol{f}_r^p$, while $-(\boldsymbol{M}\ddot{\hat{\boldsymbol{U}}} + \boldsymbol{C}_c\dot{\hat{\boldsymbol{U}}} + \boldsymbol{M}_c\hat{\boldsymbol{U}})$ is a nodal force vector generated from $\boldsymbol{f}_d^p$.

The D'Alembert inertial forces in Eq. (39) can be rewritten as a combination of space-dependent and time-dependent terms as

$$\boldsymbol{f}_r^p = -m^p\begin{bmatrix} 1 & 0 & 0 & 0 & z & -y & 0 & -x & -x & y & 0 & z \\ 0 & 1 & 0 & -z & 0 & x & -y & 0 & -y & x & z & 0 \\ 0 & 0 & 1 & y & -x & 0 & -z & -z & 0 & 0 & y & x \end{bmatrix}\begin{bmatrix} \ddot{r}_x \\ \ddot{r}_y \\ \ddot{r}_z \\ \dot{\omega}_x \\ \dot{\omega}_y \\ \dot{\omega}_z \\ \omega_x^2 \\ \omega_y^2 \\ \omega_z^2 \\ \omega_x\omega_y \\ \omega_y\omega_z \\ \omega_z\omega_x \end{bmatrix} \tag{41}$$

Note that $s_0^p = [x, y, z]^T$ is used in Eq. (39).

Dynamic stresses induced by the inertial forces $\boldsymbol{f}_r^p$ can be obtained as follows: First, twelve quasi-static structural analyses generate stress influence coefficients $\hat{S}_i^r (i=1, \cdots, 12)$ for unit values of time-dependent terms ($\ddot{r}_x$, $\ddot{r}_y$, $\ddot{r}_z$, $\dot{\omega}_x$, $\dot{\omega}_y$, $\dot{\omega}_z$, ω_x^2, ω_y^2, ω_z^2, $\omega_x\omega_y$, $\omega_y\omega_z$, $\omega_z\omega_x$). Second, a total dynamic stress history due to gross body motion is obtained by applying the superposition principle:

$$\begin{aligned} S^r = {} & \ddot{r}_x\hat{S}_1^r + \ddot{r}_y\hat{S}_2^r + \ddot{r}_z\hat{S}_3^r + \dot{\omega}_x\hat{S}_4^r + \dot{\omega}_y\hat{S}_5^r + \dot{\omega}_z\hat{S}_6^r \\ & + \omega_x^2\hat{S}_7^r + \omega_y^2\hat{S}_8^r + \omega_z^2\hat{S}_9^r + \omega_x\omega_y\hat{S}_{10}^r \\ & + \omega_y\omega_z\hat{S}_{11}^r + \omega_z\omega_x\hat{S}_{12}^r \end{aligned} \tag{42}$$

Dynamic stresses induced by inertial forces $\boldsymbol{f}_d^p$ due to deformation can be calculated in a similar way. First, the forces can be expressed as

$$\boldsymbol{f}_d^p = -m^p\sum_{i=1}^{m}\boldsymbol{B}_i\boldsymbol{\phi}_i^p \tag{43}$$

where m is the number of modal coordinates and $\boldsymbol{\phi}_i^p$ is the (3×1) translational mode shape vector defined at point p. Term $\boldsymbol{B}_i$ in Eq. (43) is the (3×3) time-dependent matrix, which can be expressed as

$$\boldsymbol{B}_i = (\tilde{\boldsymbol{\omega}}\tilde{\boldsymbol{\omega}} + \dot{\tilde{\boldsymbol{\omega}}})a_i + 2\tilde{\boldsymbol{\omega}}\dot{a}_i + \ddot{a}_i\boldsymbol{I} \tag{44}$$

where matrix $\boldsymbol{I}$ is a (3×3) identity martix.

Second, with the flexible inertial loads distributed at all nodes to which masses are lumped, given in Eq. (43), quasi-static structural analyses generate the stress influence coefficients $\hat{S}_{ijk}^d$ for the unit values of each term $(\boldsymbol{B}_i)_{jk}$ $(i=1, 2, \cdots, m$ and j & $k=1, 2, 3)$. For example, $\widehat{S}^d_{111}$ is obtained in the case that $(\boldsymbol{B}_1)_{11}=1$ and all other elements of matrix $\boldsymbol{B}$ are zero. Therefore, the total dynamic stress history from these deformational inertial forces is obtained as

$$S^d=\sum_{i=1}^{m}\sum_{j=1}^{3}\sum_{k=1}^{3}(\boldsymbol{B}_i)_{jk}\widehat{S}^d_{ijk} \tag{45}$$

According to Eq. (45), a total of $9m$ sets of finite element structural analyses (FEA) and superpositions are required for the computation of dynamic stresses from the inertial forces due to deformation.

4.2 Dynamic stress by body force and concentrated traction forces

Dynamic stresses can also be caused by externally applied body force $(\boldsymbol{F}_f)$ and concetrated traction forces $(\boldsymbol{F}_T)$ that include applied concentrated and constraint reaction forces. If these loads are expressed in the body reference frame, each stress influence coefficient can be computed for each unit magnitude load in each coordinate direction. For the applied body force, the stress influence coefficient is computed in the same way as has been done for the inertial translational load because both are distributed loads. For applied concentrated and constraint reaction loads, a stress influence coefficient is computed for the unit magnitude load in each coordinate direction, and then the stress is obtained by multipling the actual magnitude of the load.

After the stress influence coefficient associated with each unit load is defined, the total dynamic stress history S^f resulting from applied and constraint reaction loads is obtained as

$$\begin{aligned} S^f=&\sum_{i}^{naf}(\boldsymbol{F}_{axi}\widehat{S}^f_{axi}+\boldsymbol{F}_{ayi}\widehat{S}^f_{ayi}+\boldsymbol{F}_{azi}\widehat{S}^f_{azi})\\ &+\sum_{j}^{ncf}(\boldsymbol{F}_{cxj}\widehat{S}^f_{cxj}+\boldsymbol{F}_{cyj}\widehat{S}^f_{cyj}+\boldsymbol{F}_{czj}\widehat{S}^f_{czj})\\ &+\boldsymbol{F}_{fx}\widehat{S}^r_1+\boldsymbol{F}_{fy}\widehat{S}^r_2+\boldsymbol{F}_{fz}\widehat{S}^r_3 \end{aligned} \tag{46}$$

for body force $\boldsymbol{F}_f$, applied concentrated loads $\boldsymbol{F}_a$, and constraint reaction loads $\boldsymbol{F}_c$, where naf and ncf are number of applied and constraint reaction loads, repectively. The subscripts x, y, and z denote each body coordinate axis.

4.3 Overall computational procedure

Figure 2 shows the overall computational procedure and conceptual data flow for the proposed method, based on the derivations of the previous sections. First, a flexible multibody dynamic anaysis generates time-dependent terms, such as gross body motion, modal displacements, and constraintd reaction loads. Note that only a truncated set of basis vectors are used to describe the elastic deformation field of a flexible body in this simulation. Second, stress influence coefficients are computed in association with each unit value of time-dependent terms by quasi-static structural analyses. Last, the total dynamic stress is obtained by the superposition principle.

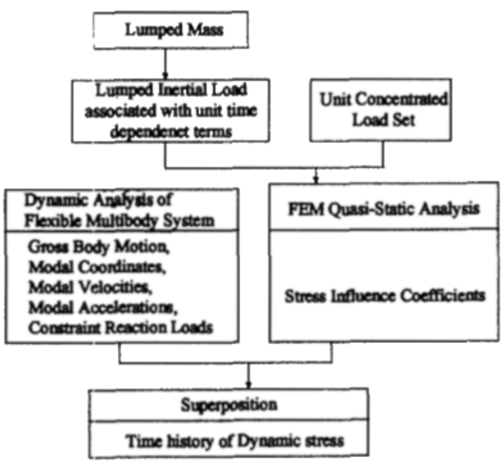

Fig. 2 Overall computational procedure

5. Numerical Example

In this section, the flexible planar four-bar mechanism in Fig. 3 and Table 1 is simulated in

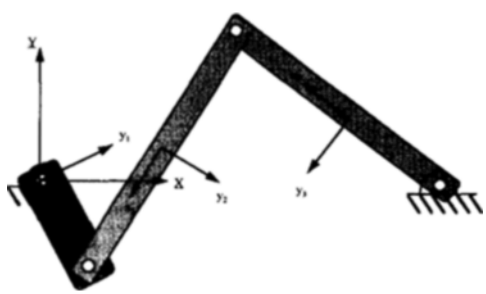

Fig. 3 Planar four-bar crank-rocker mechanism

Table 1 Four-bar mechanism parameters

Parameters	Crank	Coupler & Follower
Area	$1.07\times10^{-4}\mathrm{m}^2$	$4.065\times10^{-5}\mathrm{m}^2$
Length	$1.080\times10^{-1}\mathrm{m}$	$2.794\times10^{-1}\mathrm{m}$
Bending Moment of Inertia	$1.62\times10^{-10}\mathrm{m}^4$	$8.673\times10^{-12}\mathrm{m}^4$
Distance between ground pivots		0.254m
Lumped mass of the bearing assembly at the crank-coupler connection		0.443N
Lumped mass of the bearing assembly at the coupler-follower connection		0.368N
Modulus of Elasticity		7.10×10^7 kPa
Weight Density		$2.66\times10^4\mathrm{N/m}^3$

order to show the detailed computational procedure of the proposed method. This linkage system was tested by Turcic and others (1984b) and is chosen here to verify the simulated results. Even though four-bar mechanisms are relatively small scale, compared to real mechanical systems, they can be used to investigate dynamic characteristics of general flexible mechanical systems.

Dynamic stresses at the midspan of the coupler are calculated while the crank rotates at 340 rpm. The coupler and follower links are modelled as flexible beams and the crank is modelled as a rigid link because the crank stiffness is much higher than those of other two links. Two normal modes for each flexible beam are obtained from the simply supported boundary conditions and are used in flexible multibody dynamic simulations. For the purpose of comparison with experimental results, steady state solutions after the crank rotates four cycles are sought. To obtain steady-state solutions, an approximate damping ratio of 0.03 for every modes was used (Turcic et al, 1984b)

For the proposed method, the stress influence coefficients are generated by static structural analyses with simply supported boundary conditions. Note that any boundary conditions that will give a statically determinate system can be used in static analyses because the load system is self-equilibrated. For a slender beam with planar motion in the x-y plane, the influence coefficients are defined for; (i) the gross body motions, $\ddot{r}_x$, $\ddot{r}_y$, $\dot{\omega}_z$, and ω_z^2; (ii) a longitudinal joint reaction force at the roller end; and (iii) the forces resulting from deformation. Then the total dynamic normal stress at the extreme fiber point p is given by

$$\sigma_{xx}^p=\sigma_{xx1}^p+\sigma_{xx2}^p+\sigma_{xx3}^p \tag{47}$$

where σ_{xx1}^p, σ_{xx2}^p, and σ_{xx3}^p are normal stresses resulting from the gross body motion, joint reaction force, and deformation, respectively. They are defined as

$$\sigma_{xx1}^p=(\ddot{r}_x-g_x)\hat{S}_1^r+(\ddot{r}_y-g_y)\hat{S}_2^r+\dot{\omega}_z\hat{S}_3^r+\omega_z^2\hat{S}_4^r \tag{48}$$

$$\sigma_{xx2}^p=f_x^c S_1^f \tag{49}$$

$$\sigma_{xx3}^p=\sum_{i=1}^{m}(-a_i\dot{\omega}_z-2\dot{a}_i\omega_z)\hat{S}_i^d+\sum_{i=1}^{m}(\ddot{a}_i-a_i\omega_z^2)\hat{S}_{i+m}^d \tag{50}$$

where a_i is the i-th deformation modal displacement; $\hat{S}$ are normal stress influence coefficients; and g_x, g_y, and f_x^c are x-, y-components of the gravitational acceleration, and x-component constraint reaction force, respectively.

For the modal stress superposition method, the normal stress of Euler beam is defined as

$$\sigma_{xx}^p=E\varepsilon_{xx}^p=-E\left(\frac{h}{2}\right)\sum_{i=1}^{m}\left(\frac{d^2\phi_i}{dx^2}\right)a_i \tag{51}$$

where ε_{xx}^p is the modal strain at point p, E is the elastic modulus, h is the height of the beam, and ϕ_i is the i-th orthonormalized bending mode shape function. Note that the modal coordinate time histories are generated from the flexible dynamic simulation.

Figure 4 shows the normal stresses at the upper extreme fiber of the midspan. This figure shows that dynamic stresses computed by the proposed

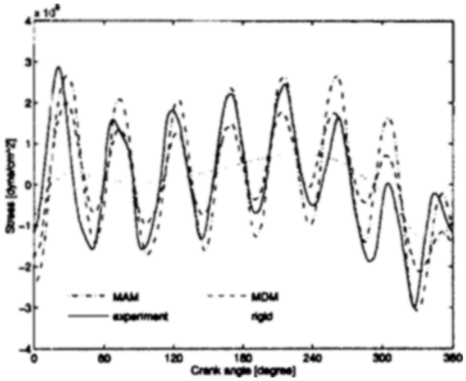

Fig. 4 Stresses at midpoint of the coupler

method are more accurate than those from the modal stress superposition method and the rigid body dynamic simulation combined with quasi-static finite element method.

6. Conclusions

An efficient method to improve the computational accuracy of dynamic stresses of the nonlinear flexible multibody dynamic system is developed. This method is so general that it can be applied to any three dimensional flexible multibody systems. It is shown that the proposed method improves dynamic stresses compared with solutions that are obtained by the modal stress superposition method and the rigid body dynamic simulation combined with quasi-static finite element method. Only a small amount of additional effort is needed to improve the accuracy of dynamic stresses by solving the mode-acceleration equations in the postprocessing stage. A numerical example of a flexible four-bar mechanism shows the effectiveness of the proposed method.

Acknowledgment

This work was supported by the basic research fund from Kwangju Institute of Science and Technology (K-JIST).

References

Bisplinghoff, R. L., Ashley, H. and Halfman, R. L., 1955, *Aeroelasticity*, Addison-Wesley, Reading, MA.

Cornwell, R. E., Craig, Jr., R. R. and Johnson, C. P., 1983, "On the Applicatin of The Mode-Acceleration Methods to Structural Engineering Problems," *Earthquake Engineering and Structural Dynamics*, Vol. 11, pp. 679~688.

Craig, Jr., R. R., 1981, *Structural Dynamics: An Introduction to Computer Methods*, John Wiley & Sons Inc., New York, NY.

Craig, Jr., R. R. and Bampton, M. C. C., 1968, "Coupling of Substructures for Dynamic Analysis," *AIAA Journal*, Vol. 6, pp. 1313~1319.

Craig, Jr. R. R. and Chang, C. J., 1977, "On the use of attachment modes in substructure coupling for dynamic analysis," *Dynamic & Structural Dynamics, AIAA/ASME 18th Structures, Structural Dynamics & Material Conference.*

Hansteen, O. E. and Bell, K., 1979, "On the Accuracy of Mode Superposition Analysis in Structural Dynamics," *Earthquake Engineering and Structural Dynamics*, Vol. 7, pp. 405~411.

Léger, P. and Wilson, E. L., 1988, "Modal Summation Methods for Structural Dynamic Computations," *Earthquake Engineering and Structural Dynamics*, Vol. 16, pp. 23~27.

Liu, T. S, 1987, "Computational Methods for Life Prediction of Mechanical Component of Dynamics Systems," Ph. D. Dissertation, The Univ. of Iowa.

Maddox, N. R., 1975,. "On the Number of Modes Necessary for Accurate Response and Resulting Forces in Dynamic Analysis," *Journal of Applied Mechanics*, pp. 516~517.

Nagarajan, S. and Turcic, D. A., 1990, "Lagrangian Formulation of the Equations of Motion for Elastic Mechanisms With Mutual Dependence Between Rigid body and Elastic Motion. Part Ⅰ & Ⅱ," *Journal of Dynamic Systems, Measurement, and Control*, Vol. 112, pp. 203~224.

Sadler, J. P an Sandor, G. N., 1973, "A Lumped Parameter Approach to Vibration and Stress Analysis of Elastic Linkages," *Journal of Engineering for Industry*, Vol. 95, No. 4, pp. 549~557.

Thomson, W. T., 1972, *Theory of Vibration* *with Applications*, Prentice-Hall, Englewood Cliffs, NJ.

Turcic, D. A. and Midha, A., 1984a, "Generalized Equations of Motion for the Dynamic Analysis of Elastic Mechansim Systems," *Journal of Dynamic Systems, Measurement, and Control*, Vol. 106, pp. 243~248.

Turcic, D. A., and Midha, A., 1984b, "Dynamic Analysis of Elastic Mechanism Systems. Part Ⅱ: Experimental Results," *Journal of Dynamic Systems, Measurement, and Control*, Vol. 106. pp. 255~260.

Williams, D., 1945, "Dynamic Loads in Aeroplanes Under Given Impulsive Loads with Particular Reference to Landing and Gust Loads on a Large Flying Boat," *Great Britain RAE Reports* SME 3309 and 3316.

Winfrey, R. C., 1971, "Elastic Link Mechanism Dynamics," *Journal of Engineering for Industry*, Vol. 93, No. 1, pp. 268~272.

Wu, S. C., Haug, E. J. and Kim, S. S., 1989, "A Variational Approach to Dynamics of Flexible Multibody System," *Journal of Mechanics of Structures and Machines,* Vol. 17, No. 1, pp. 3~32.

Yang, Z. and Sadler, J. P., 1990, "Large-Displacement Finite Element Analysis of Flexible Linkages," *Journal of Mechanical Design*, Vol. 112, pp. 175~182.

Yim, H. J. and Lee, S. B., 1996, "An Intergrated CAE System for Dynamic Stress and Fatigue Life Prediction of Mechanical System," *KSME Journal*, Vol. 10, No. 2, pp. 158~168.

Yoo, W. S. and Haug, E. J., 1986, "Dynamics of Articulated Structures, Part Ⅰ: Theory," *Journal of Structural Mechanics*, Vol. 14, No. 1, pp. 105~126.